American Mineralogist
Vol. 57, pp. 779–796 (1972)

A CONTRIBUTION TO THE CRYSTAL CHEMISTRY OF MELANOPHLOGITE

LUBOR ŽÁK, *Department of Mineralogy, Geochemistry, and Crystallography, Charles University, Prague 2, Czechoslovakia*

ABSTRACT

Melanophlogite from the second occurrence at Chvaletice, Bohemia, forms colorless cubes on lussatite in a vein cavity in a metamorphosed sedimentary pyrite-rhodochrosite deposit of Algonkian age. Fine growth zoning is parallel to the cube faces which represent bases of tetragonal sectors, composing each cube. The superstructural unit cell has space group $P4_2/nbc$, $a = 26.82$, and $c = 13.37$ Å. It breaks down by heating at 1,050°C to a cubic unit cell with space group $P4_232$ and $a = 13.4$ Å. The typical jet black color appears, but no carbon particles can be observed even at greatest magnifications. Emission spectrography indicates only Si in substantial quantity. Electron microprobe, activation, and microchemical analyses lead to a unit cell content that can be formulated as $46\ SiO_2 \cdot C_{2.2}H_{17.3}O_{5.4}S_{0.1}$. The sulfur content is much lower than that in the Sicilian melanophlogite. The clathrate structure, suggested by Kamb (1965) for melanophlogite, can be also applied for the Chvaletice mineral. Compounds of the minor elements, indicated by the formula, are framework-cavity guests and a probable cause of the tetragonal superstructure.

INTRODUCTION

The existence of melanophlogite, a cubic polymorph of silica, was confirmed only recently on material from the first occurrence of this mineral, Racalmuto in Sicily (Skinner and Appleman, 1963). Subsequent studies (Kamb, 1965; Appleman, 1965) have revealed that it is a clathrate-type compound, enclosing organic and other molecules in large polyhedral framework cavities.

A unique sample with melanophlogite was found by the mineral collector M. Duchoň in the Chvaletice deposit, eastern Bohemia, during the mining period 1964–65. Owing to its external appearance it was regarded as fluorite and kindly placed at the author's disposal for study. Preliminary optical, spectrographic, and X-ray investigations revealed its identity with melanophlogite.

The mineral assemblage containing melanophlogite (Žák, 1967) forms a vein in the metamorphosed pyrite-rhodochrosite deposit of the Algonkian Ore-Formation (Svoboda and Fiala, 1951). Melanophlogite cubes (Fig. 1) overlie a one-millimeter of layer transparent bluish-white lussatite (Žák, 1968). Under magnification tiny lussatite spherulites are commonly observable on melanophlogite crystals. The lussatite layer encrusts colorless dolomite crystals, under which minute

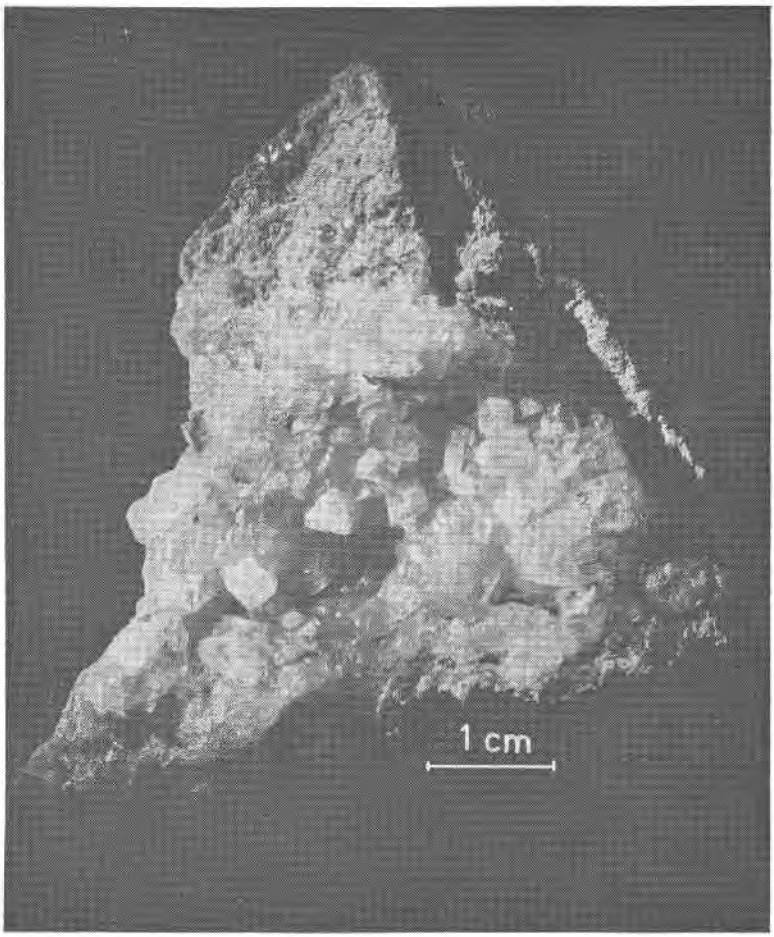

FIG. 1. Cubes of melanophlogite in a druse cavity. Photo by V. Šilhan.

pyrite crystals occur locally. Then follow layers of pinkish, concentrically-zoned rhodochrosite (X mm), pyrite (1 mm), and a fine grained pyrite-marcasite-apatite aggregate (5 mm). The lussatite is microscopically radial-fibrous and its medium index of refraction is 1.44_5. By X-rays a strongly disordered low cristobalite was established, alterable to an ordered low cristobalite after heating at 1,600°C for 10 hours (see Flörke, 1956).

PHYSICAL PROPERTIES

Morphology and Optical Properties

The cubes of melanophlogite are isolated or grow irregularly together.

Exceptionally, indications of penetration twins according to (111) were observed (see von Lasaulx, 1876). The surface of colorless transparent crystals is dull white and covered by a light brown limonite coating, easily dissolved by dilute acids. The whitish central (Žák, 1967) and other parts of crystal faces exhibit a remarkable skeletal growth (Fig. 2). Similar growth forms had been found in the Sicilian melanophlogite (von Lasaulx, 1876).

Microscopically, the melanophlogite powder is colorless and isotropic. By combination of immersion and refractometric methods, $n_{Na}^{25} = 1.457$ was determined. Sections parallel to the cube faces reveal a thin weakly anisotropic rim around a very weakly anisotropic to isotropic center. Similar observation was reported by Zambonini (1906) on melanophlogite from Giona, Sicily. The birefringence of the marginal zone of the Chvaletice mineral gradually decreases from the boundary with the core towards the cube faces. Thicker sections (~1 mm) reveal both in the rim and in the core fine zoning, parallel to the cube faces (Fig. 3), and triangular sectors that resemble six tetragonal pyramids composing one cube of Sicilian melanophlogites

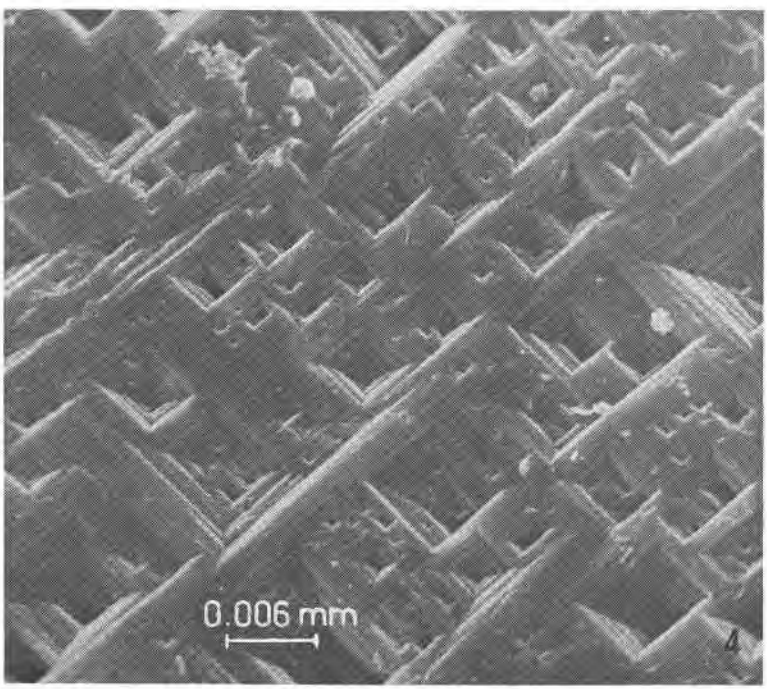

FIG. 2. Skeletal structure of a melanophlogite cube face, as seen by scanning electron microscope. Gold coated. Photo by A. Klatt, Bochum.

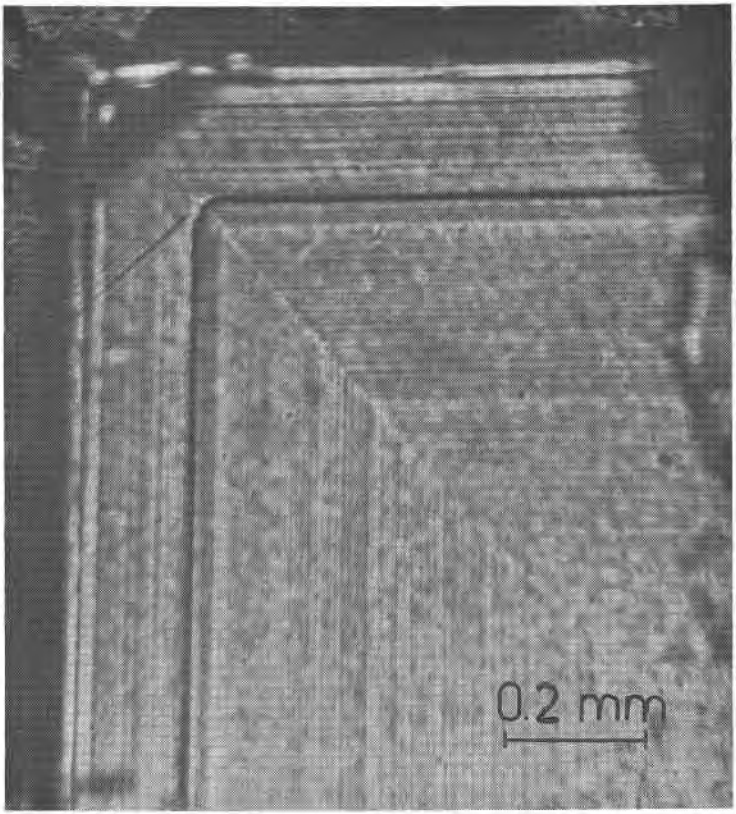

FIG. 3. Fine growth zoning. Boundaries between two sectors and between the rim and the core (dark heavy line) are clearly visible. Section, parallel to a cube face, the anisotropic margin of which was polished off. Universal stage, polarizer only.

(Bertrand, 1880; Friedel, 1890; Skinner and Appleman, 1963). The sectors in the central parts of the crystals are very weakly birefringent with transitions to optical isotropy in places (Fig. 4). The extinction of the whole cube section is parallel to the cube edges. The optical axis of the anisotropic outer zone of each sector is perpendicular to {001}, which is indicated between crossed nicols by isotropy for the light propagating in this direction. No conoscopic figure can be obtained (see also Friedel, 1890; Zambonini, 1906). Finally, thin lamellae, differing in birefringence from their vicinity, or dark lines only, are seen parallel to {110} (Fig. 4). They intersect the rim and core boundary in some cases. The extinction of them is, again, conformable with that of the whole sector. No fluorescence was observed in the

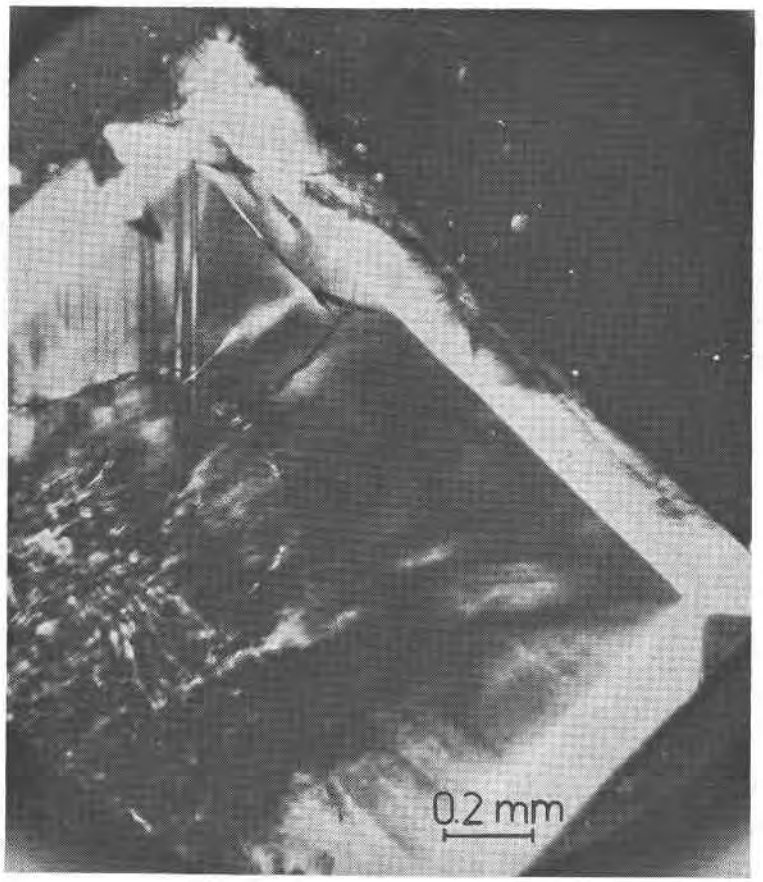

FIG. 4. Anisotropy pattern of the section from Fig. 3. Universal stage, nicols crossed. Position of a maximum birefringence in all parts of the section.

Chvaletice melanophlogite in short (254 nm) and long-wave (366 nm) ultra-violet light.

Density

A density determination was made by suspension in Klein solution diluted by water, the liquid density being measured with a Mohr-Westphal balance. Three fragments, about one millimeter in size, including the marginal zone, were used. The limonitic coating was removed by washing with hot nitric acid and distilled water. The density determined at 21°C is 2.00_5 g cm^{-3}.

Microhardness

Vickers' microhardness was determined by the Durimet (Leitz-Wetzlar) microscope. The load was 100 g, duration of the test 10 sec. A carefully polished section of melanophlogite, parallel to the cube face, and a nonoriented section of quartz from Chvaletice, mounted simultaneously in an epoxy resin block, were examined. Average values of ten measurements are 680 (range 649 to 724) kg mm^{-2} in melanophlogite and 1,330 (range 1,310 to 1,427) kg mm^{-2} in quartz. The Vickers' hardness number for melanophlogite corresponds approximately to 6.5 on the Mohs' scale (Zussman, 1967), which is in a good agreement with the value for the Sicilian material of 6.5–7 (von Lasaulx, 1876).

Thermal Behavior

After heating in air to a red glow for one minute or in an electric furnace at 800°C for three hours, the melanophlogite fragments became smoky brown in color. The previously anisotropic marginal zone became more intensively colored than the core, and turned isotropic. The intensity of the rim coloring increases towards the contact with the central part. In the Sicilian melanophlogite, observed on the heating stage (Zambonini, 1906), a colorless birefringent rim got nearly isotropic at 150°C in one case, and darkening of yellow-brown zones in the core occurred at different temperatures from 200 to 300°C. The color, zonal structure, and likely also the differences in darkening temperatures were ascribed to an organic pigment. After heating the Chvaletice mineral at 1,050°C for six hours, the crystal fragments, including both rim and core, turned jet black. They were opaque in thin section, with isotropic brown translucent or transparent edges. No heterogeneous carbon particles could be observed even at the greatest magnification of the microscope (1,600 X), contrary to the Sicilian melanophlogite (Skinner and Appleman, 1963). In powder preparations, translucent fragments show frequently brown and almost opaque narrow zones, rarely intersecting at an angle of about 120°. They can be correlated with the above-mentioned zoning and lamellae.

Infrared Absorption Spectrography

Absorption bands, characterizing unheated and heated melanophlogites, are presented in Figure 5. Non-aromatic hydrocarbons or their derivatives are suggested absorptions between 2,800 and 3,000 cm^{-1} (curve 1) disappearing after heating (curve 3), but proof is lacking. In some of other runs (*e.g.* curve 2) the mentioned absorptions were not

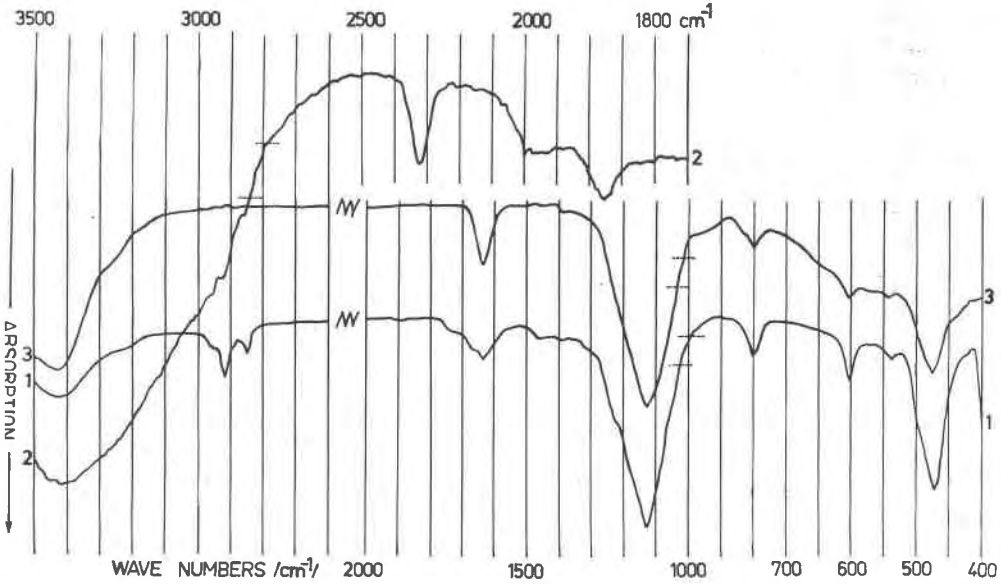

FIG. 5. Infrared absorption spectra. Hand picked mineral fragments, washed in hot hydrochloric acid and distilled water, were very finely powdered. KBr tablets, concentration of melanophlogite (curve 1 and 3) 0.2–0.3 percent. Curve 1: unheated melanophlogite, UR 10 Zeiss spectrograph. Curve 2: another sample, 621 Perkin-Elmer spectrograph. Curve 3: heated melanophlogite at 1,050°C for 6 hours, UR 10 Zeiss spectrograph. The dotted horizontal lines, transecting the curves, denote the 20–30% absorption interval.

so clearly detectable, so that organic contamination could be present. Water molecules as framework cavity guests are uncertain, though the absorption at 1,630 cm^{-1} was also found by the Nujol technique in a sample dried at 120°C for 1 hour and immediately transferred into the Nujol paste. Water remaining adsorbed on the powder particles cannot be excluded.

X-ray Crystallography

The powder pattern (Table 1) contains a number of weak diffractions that cannot be indexed by a cubic 13 Å unit cell (Skinner and Appleman, 1963), and that indicate the presence of a superstructure with a doubled cell edge. This is confirmed by single crystal methods. Rotation photographs were made with a thin section (~0.2 mm) parallel to a cube face, after polishing and cutting off the anisotropic rim. This core section was prepared from the other half of the crystal, used for optical study (Figs. 3 and 4). The section was nearly

isotropic under universal stage observation. With rotation axes parallel to the plane of the section ([100] and [010]), the X-ray photographs are identical and show weak layer lines indicating doubled cell edges. With [001] rotation axis, only extremely weak reflections of these layer lines are obtained. Rotation photographs of a marginal zone section give similar results. The photographs indicate a common tetragonal supercell (axial ratio 2:2:1 relative to the 13 Å subcell) with vertical axis perpendicular to the plane of the thin section. This cell is confirmed and specified by equi-inclination Weissenberg photographs of the core section and cube edge fragments.

Survey of the Photographs Made

	Rotation axes[1]			
	Core section		Edge fragment	
Layer line	[100]	[010]	[001]	[100]
0	+	+	+	+
1	+		+[2]	+
2	+			+
3	+			+
11				+

The photographs can be evaluated by the same tetragonal cell, the only difference being in the proportion of three orientations of intergrown cells in the X-rayed region. Whereas the edge fragments produce diffractions of a considerable intensity from two or three cell orientations with perpendicular *c*-axes, the core section demonstrates a prevalence of only one orientation of the cell. Therefore, the edge-fragment photographs are difficult to interpret in terms of a tetragonal cell, which is clearly confirmed by the core section photographs (Fig. 6). High-angle diffractions, e.g. 32.0.0 and 0.0.16 (indices relative to the 2:2:1 cell), demonstrate a difference of the corresponding interplanar spacings. The presence of the reflection 34.0.0 and the absence of an analogous 00*l* diffraction indicates doubling of the larger 13 Å subcell edge only. The photograph with the [001] rotation axis contains both 32.0.0 + 34.0.0 and 0.32.0 + 0.34.0 diffractions, with equal reflection angles in each pair of corresponding reflections.

The supercell dimensions $a = 26.82 \pm 0.03$ Å and $c = 13.37 \pm 0.02$

[1] Indices relative to the prevailing orientation of the supercell.

[2] Comparable with second layer lines of photographs with [100] and [010] rotation axes.

Å were calculated from the 32.0.0 and 0.0.16 diffractions of a Weissenberg photograph (core section), calibrated by silicon (a = 5.43054 Å.

The photographs of the higher layer lines with [100] rotation axes display considerable differences in intensities of *hkl* and *lkh* reflections, in accordance with the tetragonality of the cell. The odd layer lines (exposures up to 100 hours) show weak diffractions with two odd indices (Fig. 7) relative to the axial ratio 2:2:2, confirming the 2:2:1 supercell (see also Pyatenko, 1967). No diffractions with three odd indices have been found.

The three orientations of the tetragonal supercell with perpendicular vertical axes produce splitting of high angle reflections, both in even and odd layer lines. The most striking are doubled reflections 32.0.0 + 0.0.16 in the photographs of the edge fragments. Weak reflections of a different cell orientation are obtained also in the photographs of the central section (Fig. 6). Some diffractions, *e.g.*, 32.12.0, 12.0.16, and 32.0.6, should form triplets. Only doublets have been observed on the photographs. This can be explained by: (a) Only two prevailing orientations of the cell in the X-rayed region of the crystal, or, (b) In

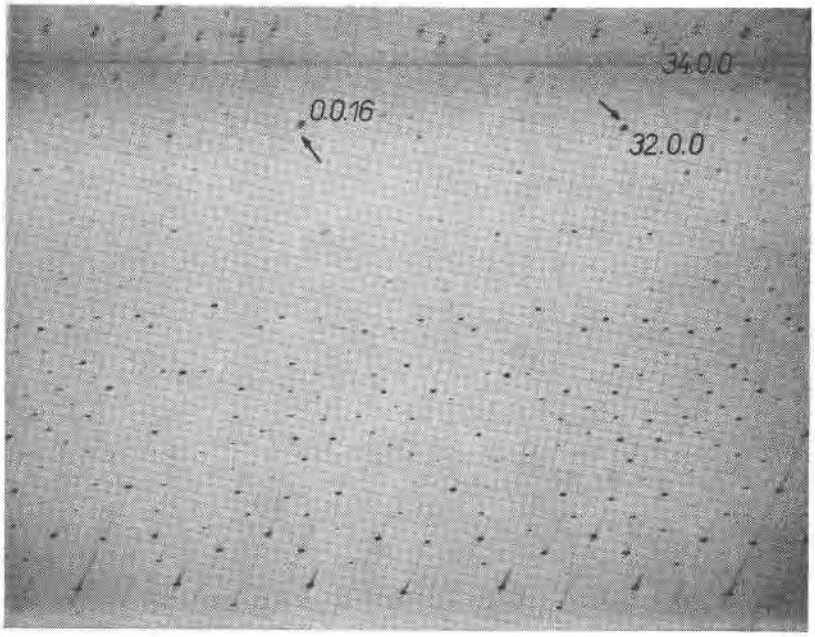

FIG. 6. Zero layer *h0l* Weissenberg photograph, core section of the unheated melanophlogite. Note the 32.0.0, 34.0.0, and 0.0.16/α_1 + α_2/reflections of the prevailing cell. Another orientation of the cell produces weak diffractions only: 32.0.0 α_1(arrow) and 0.0.16α_2(arrow). Cu/Ni radiation, exposure 52 hours.

Table 1. X-ray powder diffraction data for melanophlogite[a]

I[b]	$d_{obs.}$	$d_{calc.}$	hkl[c]	I	$d_{obs.}$	$d_{calc.}$	hkl
3	9.49 Å	9.472 Å	220 201	3	2.680	2.679	10.0.0 860 803 604
4	6.70	6.698	400 002				
10	5.99	5.990	420 401 202	1	2.666	2.666	941 922 815 762 743 614
7	5.471	5.469	421 222				
2	4.238	4.236	620 601 203	2	2.630	2.627	10.2.0 10.0.1 861 823 624 205
1	4.179	4.184	611 432 213				
6	5.862	5.867	442	3	2.615	1.614	10.1.1 852 544 215
1	3.829	3.827	631 323				
3	3.716	3.715	640 602 405	2	2.568	2.566	833 634
				5	2.487	2.487	10.4.0 10.0.2 862 845 644 405
9	3.580	3.580	641 622 423				
2	3.350	3.349	800 004				
6	3.248	3.249	801 642 443 204	1	2.392	2.396	10.3.2 853 654 455
1-?	3.220[d]	3.225	811 741 722 214	2	2.369	2.368	880 804
5	3.158	3.157	821 660 603 224	1-	2.362	2.359	11.2.1 10.5.1 872 814 744 525
2	3.052	3.053	831 652 543 324	5	2.297	2.297	10.6.0 10.0.3 863 664 605
2	2.995	2.995	840 802 404				
4	2.923	2.923	841 822 424	3	2.264	2.264	10.6.1 10.2.3 625
3	2.858	2.856	662 643				
1	2.840[d]	2.840	921 832 761 723 344	4	2.234		
				1-	2.227[d]		
2	2.776	2.778	851 524	1-	2.203		
3	2.735	2.734	842 444	1	2.198		
1-?	2.710	2.706	921 770 534	4	2.172		
				1-	2.164[d]		

some other cases also by coincidence of two diffractions with a very small difference of Bragg angle. The *h0l* split reflections do not lie on central reciprocal lattice lines, as it seems from their postions in the photographs. Owing to the strongly pseudocubic character of the tetragonal 13 Å subcell and the great distortion of the reciprocal lattice geometry in the Weissenberg photographs, their maximum difference in position with respect to the central lattice lines is too small to be observed (~0.1 mm).

Table 1. Continued

I	$d_{obs.}$	I	$d_{obs.}$	I	$d_{obs.}$	I	$d_{obs.}$
3	1.998	1-	1.758	4	1.580	1-	1.460
3	1.975	1	1.745	1	1.577	2d.	1.452
1	1.971[d]	3	1.715	1	1.570	4	1.444
2	1.949	3	1.701	1-	1.565	2	1.427
4	1.934	1-	1.676	4	1.556	2	1.420
1	1.913[d]	1-	1.672	1-?	1.552[d]	4	1.411
1-	1.909[d]	3	1.661	1-	1.545	1-	1.408[d]
3	1.894	4	1.648	1-	1.543[d]	1-	1.402
1	1.840	1-	1.645[d]	2	1.535	1	1.399[d]
1	1.834[d]	2	1.624	1	1.526	2	1.388
4	1.823	2d.	1.611	2d.	1.496	3	1.366
2	1.790	4	1.601	2	1.478	3	1.352
1	1.761			2	1.469	a.s.o.	

[a]Guinier-de Wolff camera, Cu$K\alpha$ radiation, 40 kV, 25 mA, exposure 24 hours. Internal standard Si/$\underline{a}$ = 5.43054 Å/. The $\underline{d}$ values were calculated on the basis of a tetragonal supercell with a = 26.79 Å and $\underline{c}$ = 13.395 Å. Calculating for the cell derived from the Weissenberg photograph is not preferable owing to frequent coincidences due to the pseudocubic character of the tetragonal subcell.

[b]Intensities are taken from a powder pattern, made without the internal standard under the same conditions. They are visual estimates with the scale from 1 to 10 /the most dense line/; d. means diffuse.

[c]Indices inconsistent with the space group $\underline{P4_2/nbc}$ are left out.

[d]Found only in the powder pattern without the internal standard

The reflection statistics (indexing relative to the tetragonal 2:2:1 supercell) lead to the space group $P4_2/nbc$ (Nuffield, 1966): hkl present in all orders, $hk0$ with $h+k = 2n$, hhl with $l = 2n$, and $0kl$ with $k = 2n$ only.

The powder pattern (Table 1) was calculated for an average tetragonal supercell with $a = 26.79$ Å and $c = 13.395$ Å, based on a hypothetic cubic subcell with $a = 13.395$ Å. This subcell is similar in dimensions to the cubic cell of the heated melanophlogite.

Twinning

As indicated by optical and single-crystal X-ray study, the cubes of the Chvaletice melanophlogite are composed of six pyramids, whose apices meet at the center of the cube and bases represent the cube faces. The pyramids are formed by fine tetragonal tablets, growing parallel with their bases together (Fig. 3). Their vertical axis is common and perpendicular to the corresponding cube face. Similar

composite crystals were observed on melanophlogite from Sicily by Bertrand (1880), Friedel (1890), and Skinner and Appleman (1963). The adjoining pyramids and the lamellae in them probably represent some kind of twinning. Twinning of the adjoining individuals with {110} symmetry planes (relative to the cube) is not probable, owing to the tetragonal distortion of the 13 Å cubic cell, leading to a very complicated index of the symmetry plane. Twinning with {201} symmetry planes (relative to the tetragonal supercell) requires the *c*-axes of the individuals to meet at an angle of about 90°10′. No such deviation from perpendicularity could be observed in the X-ray single crystal photographs or by the microscope. In this connection it it interesting to note Friedel's (1890) observation of higher than 90° angles of the cube faces and Zambonini's (1906) observation of a tetrahexahedron of a complicated index, on the Sicilian melanophlogite crystals. A slight compression of cube corners towards the centre of the cube was observed on the Chvaletice crystals, too. The questions need further study.

Heated Melanophlogite

Small marginal-zone + core fragments were heated in air at 1,050°*C* for 12 hours. Powder and rotating crystal X-ray photographs (rotation axis [100]) revealed a breakdown of the superstructure to a cubic structure with $a = 13.4$ Å. The superstructure reflections disappeared almost completely in the Guinier powder pattern and completely in the single crystal photographs. Equi-inclination Weissenberg photographs of zero and first layer lines (Fig. 7) display a diffuse character of split reflections. Different intensities of many reflections, when compared with the corresponding ones of the unheated mineral, are observable. The reflection survey records the presence of *hkl*, *hhl*, and 0*kl* reflections in all orders and 00*l* present with $l = 2n$ only. Of the space groups $P4_232$ and $P2_13$, the group $P4_232$ is indicated by the diffraction symmetry. The space group $P4_232$ had been given for the Racalmuto melanophlogite by Skinner and Appleman (1963), but the space group $Pm3n$ was suggested later (Kamb, 1965). Contrary to the Racalmuto melanophlogite with *hhl* present only if $l = 2n$, the heated Chvaletice melanophlogite exhibits the *hhl* reflections in all orders (Fig. 8). Nevertheless, the *hh*1 reflections are weak by comparison with other reflections and the corresponding *hh*1 or *h*2*h* diffractions of the unheated melanophlogite have not been found.

Chemical Composition

Qualitative spectrographic analysis gave Si in substantial, Al, Cu,

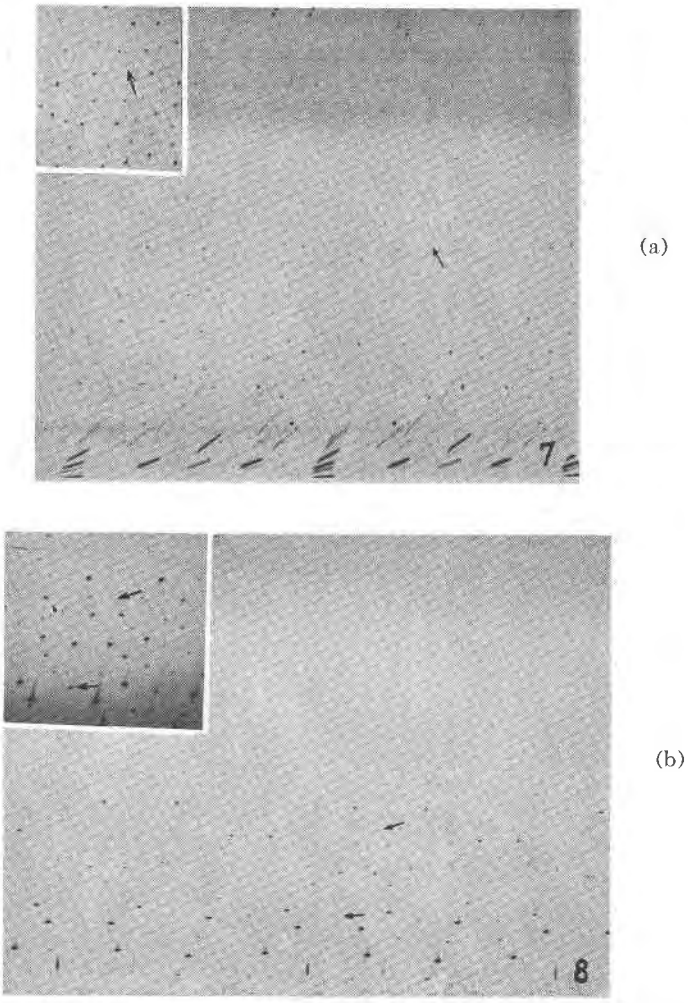

FIG. 7. Third *h3l*(a) and first *h1l*(b) layer equi-inclination Weissenberg photographs of unheated and heated melanophlogites. Edge fragments. Note the weak 23.3.0, 313, and 616 reflections (arrows). Cu/Ni radiation, exposures 60 and 33 hours. Left upper corners: detail with longer exposures.

Mg, and Mn in insignificant (<0.X percent), and Ag, Fe, and P? in trace quantities. JXA-3A electron microprobe tests for nitrogen and fluorine were negative, and only the sulfur test was slightly positive. A nitrogen content lower than 1 percent (Weinryb, 1967) probably cannot be detected under the experimental conditions used. Elements with $Z > 11$, except silicon, were not found.

Sulfur, silicon, and oxygen were determined by activation, carbon and hydrogen by microchemical methods from powdered samples, silicon and carbon by the electron microprobe.

Sulfur activation analysis (0.01 g, F. Kukula analyst) was carried out by nuclear reactor bombardment, combined with a chemical separation of the beta-active ^{35}S. The standard was ammonium sulfate. A sulfur content 0.11 ± 0.03 percent was found.

Silicon and oxygen of the sample (0.03 g) were transformed into ^{28}Al and ^{16}N radioisotopes by fast neutrons, produced in a neutron generator (J. Bartošek and I. Kašparec analysts). The standards were quartz from Chvaletice and silica glass. The average value of three measurements is 45 percent (range 43 to 46) for silicon and 53 percent (range 51 to 56) for oxygen.

For silicon analyses with a Cambridge Geoscan electron microprobe, a graphite-coated polished section (from microhardness measurements), mica crystal, accelerating voltage 20 kV, sample current 20 nA, Si$K\alpha_1$ radiation, and standard of quartz from Chvaletice were used. Carbon was measured with a Japanese JXA-3A probe (K. Stránský and A. Rek analysts), using a copper-coated section, electron beam diameter 1.8 μm, lead stearate crystal, 10 kV, 27 nA sample current, C$K\alpha$ radiation, and standards of graphite and aragonite. The wavelength shift was respected (Castaing, 1960; Kohlhaas and Scheiding, 1969) and the carbon contamination reduced by a slow sample movement (100 μm per min.). A correction for the remaining carbon contamination was made by the carbon-free quartz standard, analyzed immediately after the melanophlogite. After corrections for background and dead time, Si = 43.6 and C = 0.3 (graphite standard) or 0.6 percent (aragonite standard) were obtained. These raw data were corrected for absorption (Birks, 1963; Springer, 1967) and atomic number (Springer, 1966). A model analysis (Table 2), based on analytical data and comparison of measured and calculated densities, was used for calculation of the corrections. The C$K\alpha$ absorption coefficients for carbon (2,282) and calcium (68,502) had to be extrapolated from literature data (Henke, *et al.*, 1957). To get the same result from both standards, an antagonistic change of absorption correction factors was necessary. Finally, Si = 44.2 and C = 0.8 ± 0.4 percent were obtained.

Carbon zonality: the mentioned carbon content was found in the central part of the melanophlogite section, parallel to the cube face at a certain distance from the surface. The anisotropic rim, about 0.2 mm thick, gave higher carbon contents. Seven analyses at different places of the margin with the electron beam moving from the cube plane to

the center of the section gave from 0.8 to 1.2 percent of carbon (average 1.0 %), relative to the 0.8 percent carbon content of the central part. The carbon content was measured along 1 mm abscissae perpendicular to the zoning, the intensities of CKα radiation integrated in about 30 μm intervals. Rare anomallously high intensities in the core were attributed to section surface contamination. The optical picture of the transparent polished section used for analyses, was very similar to that depicted by Figure 4.

Microchemical analyses of carbon and hydrogen were made by a Perkin-Elmer C–H–N elemental analyser (J. Horáček analyst). The sample (0.006 g) was heated successively at 950°C for 26 min. and at 1,000°C for 23 min. in oxygen atmosphere. The elements were converted into carbon dioxide and water. The greenish yellow mineral powder after the analysis, when heated at 1,000°C for 2 hours in air afterwards, became greyish white, which indicated a nearly complete carbon liberation during the analysis. A mixture of the rim and core of the crystal gave in this way 1.06 percent carbon and 0.66 percent

TABLE 2. COMPARISON OF MELANOPHLOGITE ANALYSES

	Racalmuto[a]	*Chvaletice*
	%	%
Si	43.2	44.2[d]
O	52.6[b]	53[e]
C	1.2	0.9[f]
S	2.3	0.1[e]
H	0.81	0.6[g]
	100.11	98.8
	$\rho_{meas.} = 2.052$ g cm^{-3}	$\rho_{meas.} = 2.00_5$ g cm^{-3}
	$\rho_{calc.} = 2.06$[c]	$\rho_{calc.} = 2.001$[h]

[a] B. L. Ingram analyst (Skinner and Appleman, 1963). Oxides were recalculated to elements.

[b] Calculated from SiO_2 and SO_3.

[c] Calculated by Kamb (1965).

[d] By electron microprobe analysis.

[e] By activation analysis.

[f] Average of electron probe and microchemical analyses.

[g] By microchemical analysis.

[h] Calculated on the basis of the formula in text (4 x) and $a = 26.82$ Å, $c = 13.37$ Å ($V = 9{,}617.2$ Å^3).

hydrogen. After a correction for water and carbon dioxide (adsorption, inclusions), C = 1.0 and H = 0.6 percent.

Crystallochemical Considerations

A formula for the Chvaletice melanophlogite was calculated on the basis of the model analysis (Table 2), taking 46 silicon atoms (Kamb, 1965) in 1/4 of the tetragonal superstructural unit cell ($a = 28.82$, $c = 13.37$ Å):

$$Si_{46}O_{92} \cdot C_{2.17}H_{17.25}O_{5.42}S_{0.09} \cong 46\ SiO_2 \cdot C_2H_{17}O_5$$

Six larger tetrakaidecahedral and two smaller pentagonal dodecahedral cavities in the 13 Å unit cell of melanophlogite (Kamb, 1965; Appleman, 1965) can accommodate guest molecules without chemical bounds to the silica framework. The chemical composition of the guest molecules has not been known exactly and was discussed by Kamb (1965). In the Chvaletice mineral, the following element combinations can be present in the guest molecules: C + H ± S ± O, H + O, C + O, and S ± O ± H. According to the preceeding analytical data, non-aromatic hydrocarbons or their derivatives and water are probable and prevailing guests. Contrary to the Racalmuto melanophlogite (Skinner and Appleman, 1963), the sulfur content of the Chvaletice mineral, in accordance with its lower density and refractive index, is very low and probably unimportant for stabilization of the structure (see Kamb, 1965). The optical and thermal investigations of the Chvaletice melanophlogite especially indicate zoning of the crystals. Somewhat different physical and chemical properties are observed in the rim and the core of the crystals. No differences have been detected by X-rays, but the carbon content was found higher in the rim than in the core. Differences in occupancy of the larger and smaller framework cavities, in number of molecules in one cavity, and in frequency or chemical composition of the carbon compound guest molecules might be responsible for the property changes.

The idea of a lower than cubic symmetry of melanophlogite (Bertrand, 1880; Friedel, 1890; Kamb, 1965) was confirmed on the melanophlogite from Chvaletice. A tetragonal distortion of the cubic 13 Å cell, connected with the origin of the tetragonal superstructure, is most probably due to the guest molecules (Kamb, 1965). The importance of these guests can be seen from heating experiments. By decomposition of the organic molecules the superstructure was destroyed and the 13 Å cubic cell originated.

The Chvaletice melanophlogite originated most probably under low-temperature and low-pressure conditions, as indicated by its paragen-

esis. It crystallized in the last stage of metamorphic hydrothermal vein formation by Alpine paragenetic processes. The source of carbon was country rock sediments: Graphite schists and fine-grained rhodochrosite with graphite.

Identification of the guest molecules and a detailed knowledge of the crystal structure (Appleman, 1965) are of utmost importance and the goals of future work on melanophlogite, making its laboratory synthesis easier.

ACKNOWLEDGMENTS

Professor B. Kamb's kind efforts and helpful comments to the manuscript led to its considerable improvement, especially in further optical and X-ray work that confirmed a tetragonal, instead of the cubic supercell originally postulated. Thanks are also due to the following: M. Duchoň, Dr. V. Syneček for discussions and valuable suggestions in the X-ray study, Z. Šikýř for numerous X-ray Weissenberg photographs and calculations, Dr. Z. Johan, Dr. J. Hrušková, and Dr. M. Rieder for help in the X-ray work, Ing. J. Smolíková, Dr. L. Vašíčková, and Ass. Prof. Pavlík for IR spectra, Ing. L. Vašková for high temperature heating experiments, Dr. A. Blüml and J. Pěknic for microhardness measurements, Prof. J. Novák for discussion of structural crystallographic problems, Prof. O. W. Flörke for literature, Prof. B. Bouček for assistance in Stereoscan microphotographs, and to several others for quantitative analyses.

REFERENCES

APPLEMAN, DANIEL E. (1965) The crystal structure of melanophlogite, a cubic polymorph of SiO_2. (Abstr.) *Amer. Crystallogr. Assoc. Mineral. Soc. Amer. Joint Meet., Gatlingburg,* p. 80.

BERTRAND, EMILE (1880) Sur la thaumasite et la melanophlogite. *Bull. Soc. Franc. Mineral.* **13,** 159–160.

BIRKS, L. S. (1963) *Electron Probe Microanalysis. New York-London.* [Transl. Moskva, 1966].

CASTAING, R. (1960) Electron probe microanalysis. *Adv. Electron. Electr. Phys.* **13,** 317–386.

FLÖRKE, O. W. (1956) Zur Frage des "Hoch"-Cristobalit in Opalen, Bentoniten und Gläsern. *Neues Jahrb. Mineral., Monatsh.* **1955,** 217–333.

FRIEDEL, G. M. (1890) Sur la mélanophlogite. *Bull. Soc. Mineral. Franc.* **13,** 356–372.

HENKE, BURTON L., R. WHITE, AND B. LUNDBERG (1957) Semi-empirical determination of mass absorption coefficients for the 5 to 50 Ångstrom X-ray region. *J. Appl. Phys.* **28,** 98–105.

KAMB, BARCLAY (1965) A clathrate crystalline form of silica. *Science,* **148,** 232–234.

KOHLHAAS, ERICH, AND F. SCHEIDING (1969) Der Nachweis von Kohlenstoff mit der Elektronenmikrosonde. *Arch. Eisenhüttenw.* **40,** 47–51.

VON LASAULX, A. (1876) Melanophlogit, ein neues Mineral. Miner.-kryst. Not. VII. *Neues Jahrb. Mineral., Geol., Paleont.* **1876,** 250–257.

NUFFIELD, E. W. (1966) *X-ray Diffraction Methods.* New York-London-Sydney.

PYATENKO, YU. A. (1967) On one special case of interpretation of powder patterns. *Mineral. Sbornik L'vov. Gos. Univ.* **21,** 193–197 [in Russian].

ROST, RUDOLF (1961) *Microchemical Determination of Minerals*. Praha [in Czech].

SKINNER, BRIAN J., AND D. E. APPLEMAN (1963) Melanophlogite, a cubic polymorph of silica. *Amer. Mineral.* **48**, 854–876.

SPRINGER, G. (1966) Die Korrektur des Ordnungzahl-effektes bei der Elektronenstrahl-Mikroanalyse. *Neues Jahrb. Mineral., Monatsh.* **1966**, 113–125.

——— (1967) Die Berechnung von Korrekturen für die quantitative Elektronenstrahl-Mikroanalyse. *Fortschr. Mineral.* **45**, 103–124.

SVOBODA, J., AND F. FIALA (1951) A report on geological research near Zdechovice and Morašice in the Iron Mts. *Věst. Ústř. Úst. Geol.* **26**, 114–120 [in Czech].

WEINRYB, E. (1967) Anwendung der Röntgenstrahl-Mikroanalyse für leichte Elemente. *Microch. Acta, Suppl. II,* 173–187.

ŽÁK, LUBOR (1967) Find of pyrophanite and melanophlogite in Chvaletice (E Bohemia). *Čas. Mineral. Geol.* **12**, 451–452.

——— (1968) Melanophlogite from Chvaletice (E Bohemia). (Abstr.), *Int. Mineral. Assoc. 6th Meet., Prague,* p. 107–108.

ZAMBONINI, F. (1906) Einige Beobachtungen über die optischen Eigenschaften des Melanophlogit. *Z. Krystallogr.* **41**, 48–52.

Manuscript received, October 7, 1970; accepted for publication, December 14, 1971.